Advanced Composite Materials

Design of a hybrid composite strut tower for use in automobiles

Hyun Chul Lee[a], Yong Sik Jung[a], Hyun Ju Oh[a] & Seong Su Kim[a]

[a] Department of Organic Materials and Fiber Engineering, Chonbuk
National University, 567 Baekje-daero, Deokjin-gu, Jeonju-si,
Jeollabuk-do, Republic of Korea
Published online: 10 Jan 2014.

PLEASE SCROLL DOWN FOR ARTICLE

Taylor & Francis
Taylor & Francis Group

Design of a hybrid composite strut tower for use in automobiles

Hyun Chul Lee, Yong Sik Jung, Hyun Ju Oh and Seong Su Kim*

Department of Organic Materials and Fiber Engineering, Chonbuk National University, 567 Baekje-daero, Deokjin-gu, Jeonju-si, Jeollabuk-do, Republic of Korea

Lightweight hybrid composite strut towers for use in automobiles were designed to increase the structural rigidity and for the prevention of permanent deformation and cracking. When the suspension structure in automobiles is increased in hardness to further increase the operational performance, the strut tower, which is the mechanical part that joins with the suspension system, is easily deformed by impact forces that result from passing over road surface irregularities, such as a pothole or bump in the road. In this work, the stress distribution of a strut tower made of a carbon fiber-reinforced composite and a back-up metal was analyzed by using the finite element (FE) method, and an optimum stacking sequence of the hybrid composite for reducing the materials cost was suggested based on the FE-analysis results. The hybrid composite strut towers were fabricated, and their dynamic characteristics were analyzed by impact tests.

Keywords: strut tower; hybrid composite; carbon fiber-reinforced composites; FE-analysis; optimization

1. Introduction

The use of carbon fiber-reinforced composite materials in engineered structures has grown increasingly common due to the improved properties of these materials, including their high specific modulus and strength vs. that of conventional materials.[1] The global auto industry has made advances in the improvement of driveline efficiency and in the lightweight development of structures, increasingly using carbon fiber-reinforced composites to achieve modest weight savings.[2]

The strut tower of the automobile is the framework that provides the mounting points for the suspension. The strut tower must provide sufficient rigidity for precise handling, must absorb impact energy, and must resist static and cyclic loads, which occur as the result of interactions with the road.[3] When passing a pothole, the impact force is delivered to the strut tower through the suspension system, and permanent deformation such as 'mushrooming' or cracking can be generated in instances when the impact force exceeds the yield strength of the strut tower structure. The impact force depends on the road surface conditions, such as the surface irregularities, and on the vehicle parameters, such as the vehicle speed, the vehicle weight, and the suspension damping coefficients.[4] Colombo et al. investigated the cause of premature failure in the upper strut mount of a McPherson suspension under low-velocity conditions.[3] They found that the upper strut mount failure, which was due to an impulsive load,

---

*Corresponding author. Email: sskim@jbnu.ac.kr

could not be justified by the static and dynamic loads acting on the component, which were caused by road irregularities and vehicle maneuvering during usual working conditions.

Additionally, many previous investigations have tried to realistically describe the dynamic behavior of automotive systems through the use of appropriate mathematical models and computer simulation analyses. Ben Mrad et al. investigated the non-linear dynamic modeling of an automobile hydraulic active suspension system.[5] Minakawa et al. measured the force transmitted from the road surface to the tires and found that the force had a sharp directivity; according to their results, the force directivity was inclined rearward in side view, and the inclination angle was dependent on the vehicle velocity.[6] He et al. calculated the static stress of the spring tower caused by the body weight by using finite element (FE) modeling; they also measured strain signals of different test conditions.[7]

The strut reinforcement plates and the strut bar, which is connected to the strut tower by the use of a mechanical joint, have been used to prevent conventional damage to the strut tower. Partial mechanical joints, however, can be effective for preventing deformation in local areas around bolt joints. Adhesive bonding can be used to efficiently offer a more uniform stress distribution around the strut tower and it has other advantages, such as fatigue life extension, weight saving, and the prevention or reduction of corrosion between dissimilar materials.[8]

Fiber-reinforced composites have been applied to lightweight structures for use in vehicles due to their high specific strength and stiffness. Feraboli and Masini developed the carbon/epoxy body panels and structural components of the Lamborghini Murcielago and discussed the influence of fiber architecture on the strength of a composite panel for the same fiber/resin system.[9] Al-Qureshi designed a single-leaf, variable thickness spring of glass fiber-reinforced plastic with similar mechanical and geometrical properties to the multi-leaf steel spring and found that the composite leaf spring met the requirements of light trucks.[10]

In this study, the impact quantity of the strut tower under severe working conditions was calculated, and a FE analysis was performed to obtain the stress distributions of the hybrid composite strut tower with respect to the stacking sequence. An optimum stacking sequence was suggested based on the non-dimensionalized stress and the materials cost in combination with the FE-analysis results. The hybrid composite strut towers fabricated by carbon fiber-reinforced composites were tested for measurements of their dynamic properties, including the impact resistance, by use of an impact test.

2. Properties of the carbon fiber-reinforced composites

Two types of fiber-reinforced composite were studied, including a carbon/phenolic 8-harness satin weave composite (Hankuk fiber, Republic of Korea) and a unidirectional carbon/epoxy composite (SK chemical, Republic of Korea). The carbon/phenolic fiber-reinforced composite was a PAN (Polyacrylonitrile)-based T300, and the matrix was a resol-type phenolic matrix with 8 wt.% carbon black powder. This material is considered to improve both the fracture toughness by the addition of carbon black and the draping efficiency of the strut tower structures. The carbon/epoxy consisted of a pitch-based high stiffness carbon fiber and a bisphenol-A epoxy resin. The main role of this material was to improve the overall stiffness of the hybrid composite strut tower. Both composite materials were prepared by the layering of prepregs, followed by curing with the suggested cure cycle, as shown in Figure 1.
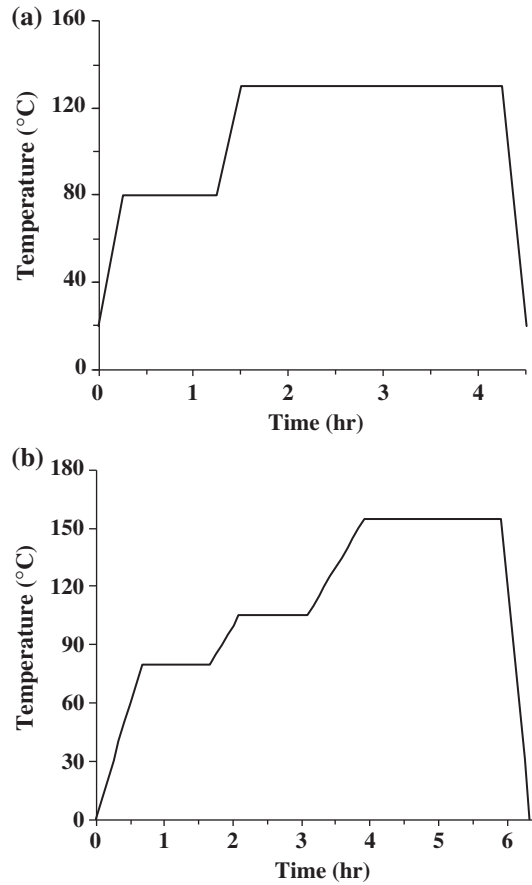
Figure 1. The manufacturer's recommended cure cycles: (a) carbon/epoxy, and (b) carbon/phenolic.

Mechanical tests, including the tensile test, the compressive test, and the Iosipescu test for shear properties, were performed to determine the engineering constants of the composite materials. Five tests were carried out for each test type, from which the average orthotropic composite mechanical properties were calculated as listed in Table 1.

3. Design of the hybrid composite strut tower

3.1. Design process

Many researchers have tried to analyze the stress distribution in car bodies by using dynamic analysis tools as the vehicle passes over either a pothole or bump on the road surface. However, it is very difficult to predict the dynamic response of the body because the dynamic characteristics of the vehicle strongly depend on the chassis system, which includes the suspension, the steering, and the tires. Therefore, structural optimization under dynamic loading conditions is required to treat large amounts of computational time for analysis and sensitivity analysis in accordance with time-dependent behaviors.[11] In this work, the design of the hybrid composite strut

Table 1. The mechanical properties of the carbon/phenolic and carbon/epoxy composites.

Materials		Weft (1)	Warp (2)	Through-thickness (3)
Carbon/phenolic 8-harness satin weave composite (Hankuk fiber, Republic of Korea), Material cost: $104.60	Tensile modulus (GPa)	50.7	73.2	14.3
	Tensile strength (MPa)	433	540	17.2
	Compressive strength (MPa)	221	264	809
	Poisson's ratio	v_{12} 0.05	v_{13} 0.21	v_{23} 0.2
	Shear modulus (GPa)	G_{12} 5.77		G_{13} 3.75
	Shear strength (MPa)	75		17.5
Unidirectional carbon/epoxy (SK chemical, Republic of Korea), Material cost: $165.20	Tensile modulus (GPa)	Longitudinal		380
		Transverse		5.1
		Shear		5.53
	Tensile strength (MPa)	Longitudinal		1500
		Transverse		65
		Shear		40
	Poisson's ratio			0.3

tower was progressed by using a static FE-analysis to improve the efficiency of the computational calculations, and the static FE-analysis of the hybrid composite strut tower was compared with the results of the impact tests and with those of the dynamic FE-analysis. The critical load (the yield point of the steel strut tower) was calculated by using static FE-analysis with ABAQUS standard/explicit, as shown in Figure 2. It was assumed that the majority of deformation in the front body was induced by bumps in the road or potholes and that this deformation occurred in the top of the strut tower; this assumption is validated by previous works.[12] Accordingly, only a portion of the strut tower was modeled to increase the overall computational inefficiency and a
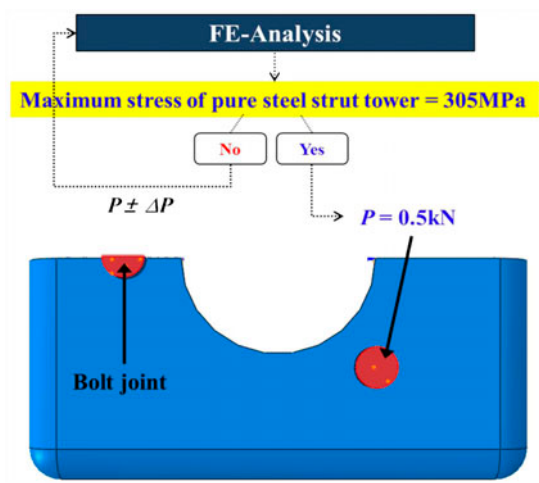

Figure 2.   An algorithm for calculating the critical load using static FE-analysis.

three-dimensional model of the steel strut tower of a commercial vehicle is shown in Figure 3(a). A symmetric boundary condition was used at the cross-section of the half-model and the three edges of the model were fixed in the z-direction because the displacement at the edge was negligible compared to that of the top of the strut tower. The static load was applied at the mechanical bolt joint located on the top of the strut tower and the analysis was repeated with respect to the load amount until the maximum stress approached the yield stress. The stress distribution of the strut tower under a load of 0.5 kN (applied to each bolt joint) is shown in Figure 3(b). A maximum stress of 307 MPa was generated around the bolt joint, and this value was close to the yield strength of hot-rolled steel.

Using several assumptions, a simple dynamic calculation was performed to estimate the impulse on the strut tower under severe working conditions. If the tire is assumed to be a perfect elastic body, it is possible to calculate the velocity change of the vehicle, ΔV, as the vehicle passes over the pothole, as shown in Figure 4(a). The calculation variables come from the conditions of a commercial medium-sized car with a weight of 1320 kg_f passing over a bump in the road at a speed of 40 km/h. The impulse can be obtained with the following equations:

$$R\cos + h = R$$

$$\cos\theta = 1 - \frac{h}{R}$$

$$\Delta V = 2V\sin\theta = 2V\sqrt{\frac{h}{R}\left(2 - \frac{h}{R}\right)} = 10.7\,\text{m/s}$$

where, R: the tire radius, h: the height of the bump or pothole, l: the length of the bump or pothole, V: the initial velocity.

It was assumed that the impulse from a collision between the tire and a bump in the road was approximately 70% absorbed by the suspension system, while the remainder reached the strut tower.[13,14] The Δt was determined from the impulse time in the strut mount while further considering the phase delay of the suspension system. The force-time curve shown in the strut tower is very similar to that depicted in Figure 4(b) because the exciting frequency due to a strong impulse comes under the high frequency range.[15] Accordingly, the maximum force can be calculated as given below:

$$\text{Impulse } I = \frac{F_{\max}\Delta t}{2} = \frac{F_{\max} \times 0.025\,s}{2} = 0.3 \times m\Delta V = 108\,\text{kg m/s}$$

$$\therefore F_{\max} = 8.64\,\text{kN}$$

3.2. *Optimizing process*

The goal in designing a hybrid composite strut tower is to reinforce the steel strut tower with a lightweight structure to prevent damage from a foreign impact force. In this study, a 30% weight reduction compared to the conventional steel strut tower was specified as a design constraint. Accordingly, the steel thickness of the hybrid composite strut tower was reduced from 1.5 to 0.6 mm. The composite thickness was also determined to satisfy the constraints, and the stacking sequences with the total thickness values and the volume ratios of the two composites are shown in Table 2 as the design
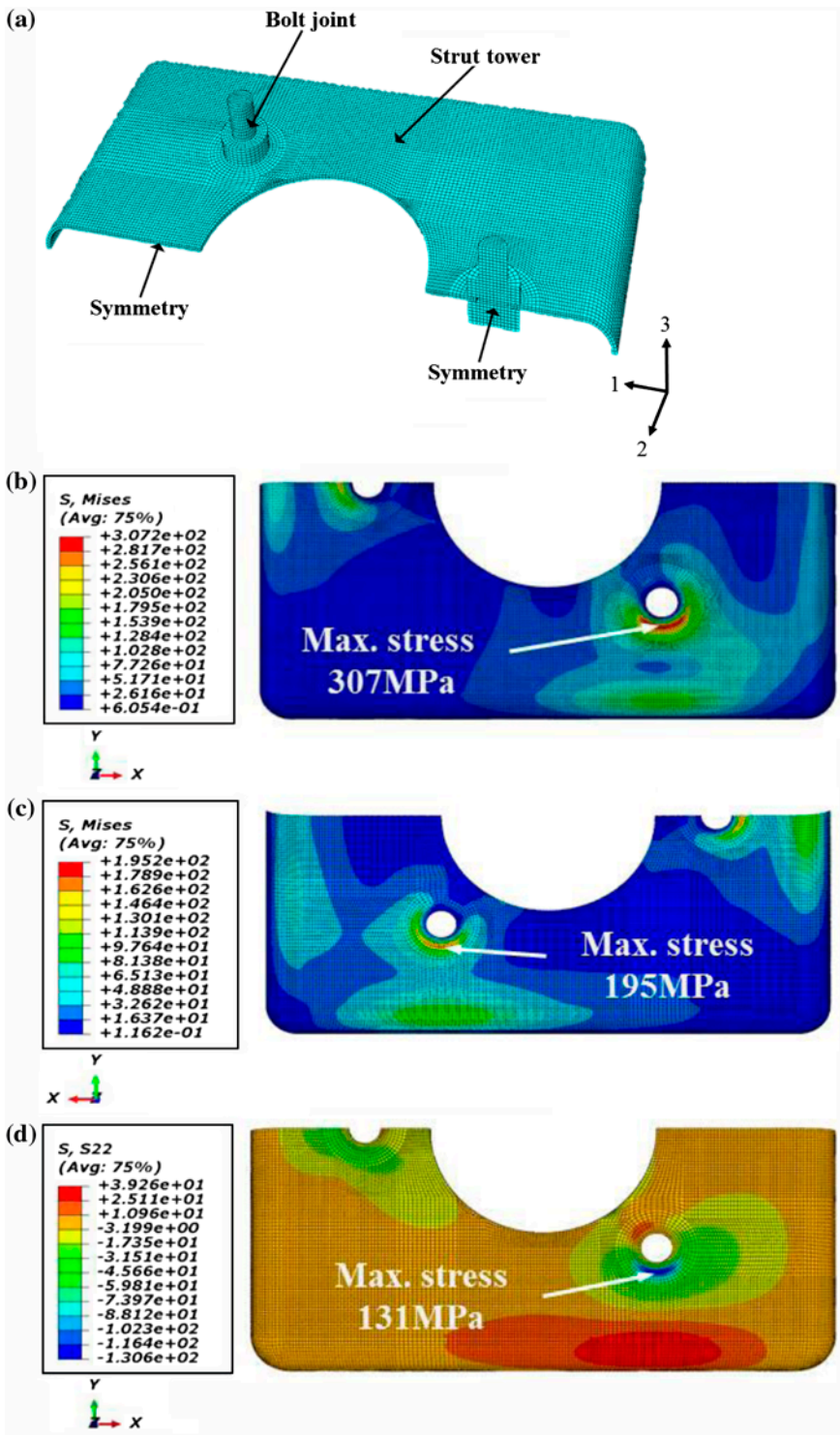
Figure 3.   The FE-modeling and stress distribution of the hot-rolled steel strut tower and the hybrid composite strut tower with a laminate stacking sequence of $[0/90/0/90]_{s,ce}$ in the static state FE-analysis: (a) the 3-D model, (b) the hot-rolled steel strut tower, (c) the steel part, and (d) the composite part.
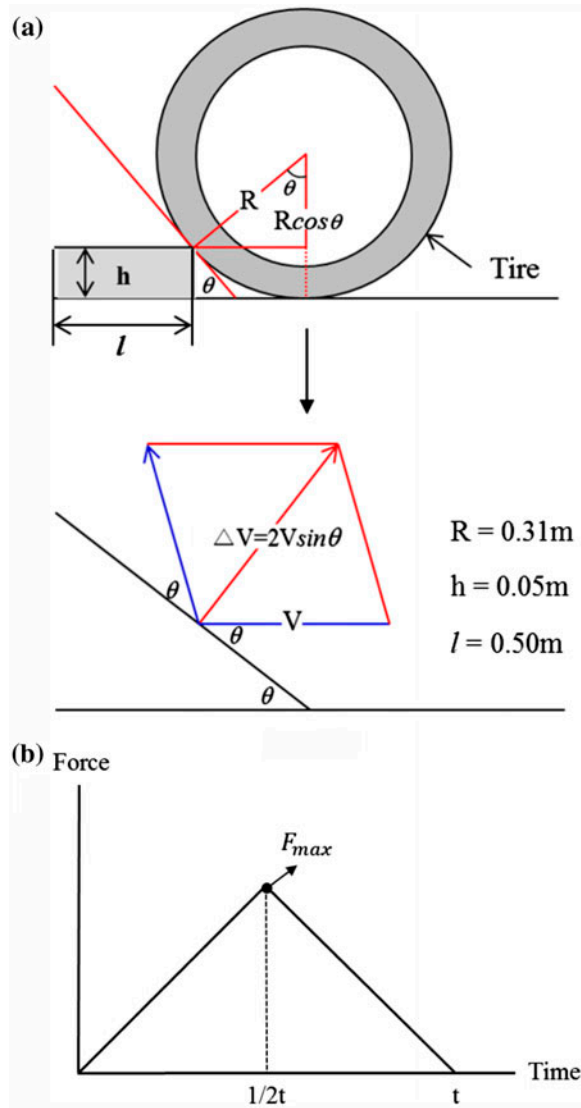
Figure 4. A simple dynamic calculation: (a) the schematic diagram used to calculate the velocity change and (b) the maximum force in the force-time curve.

parameters. The stacking sequences, whose fibers were arrayed perpendicular between subsequent layers, were selected to maximize the laminate stiffness. The laminate stiffness was calculated based on the CLPT (Classical Laminated Plate Theory).

The objectives of optimization are to minimize the stress level of the steel strut tower and to minimize the materials cost by controlling the stacking sequence. The general method for optimization is to construct the objective function with independent design parameters.[16] In this work, however, the variables were not independent because the total thickness of the composite plate was changed by the volume ratio of the carbon/phenolic and carbon/epoxy. Accordingly, a simple optimizing method for the multi-objective functions was suggested as:

Table 2. Maximum stress and materials cost with their normalized values with respect to stacking sequence.

Stacking sequence	Total thickness (mm)	CP volume (%)	CE volume (%)	Maximum stress (MPa)		Materials cost ($)	Normalized stress $(f(t, v)/f_{max})$	Normalized cost $(g(t, v)/g_{max})$	Weight-reduction (%)
				Hot-rolled steel	Composite				
$[(0/90)_{s,cp}(0/90)_{s,ce}]$	1.6	37.5	62.5	298	279	15.80	1	0.65	36.7
$[0/90/0/90/0/90]_{s,cp}$	1.8	100.0	–	289	191	11.30	0.97	0.47	36.9
$[0/90/0/90]_{s,ce}$	2.0	–	100	216	213	21.10	0.77	1.00	28.8
$[(0/90)_{s,cp}/(0/90/0)_{s,ce}]$	2.1	28.6	71.4	202	233	21.80	0.70	0.90	28.9
$[(0/90/0)_{ce}/(0/90)_{s,cp}/(0/90/0)_{ce}]$	2.1	28.6	71.4	201	237	21.80	0.69	0.90	28.9
$[(0/90)_{2s,cp}/(0/90/90/0)_{ce}]$	2.2	54.5	45.5	187	182	19.60	0.65	0.81	29.0
$[(0/90)_{ce}/(0/90)_{2s,cp}/(90/0)_{ce}]$	2.2	54.5	45.5	250	127	19.60	0.75	0.81	29.0
$[0/90/0/90]_{2s,cp}$	2.4	100	–	195	131	15.10	0.65	0.82	29.2

$$\text{Stress} = f(t, v), \ \text{Materials cost} = g(t, v)$$

$$\text{Minimize} \ \Sigma(f(t, v) + g(t, v))$$

$$\text{Subject to} \ 0 < t < t_{\max}, \quad 0 \le v \le 1$$

where, t: the total thickness of the composite part, v: the volume ratio of the carbon/phenolic and carbon/epoxy, $t_{\max}$: the maximum thickness to satisfy the weight reduction constraint.

To conduct the optimization of the hybrid composite strut tower, the base values of the stress and materials cost and the weight factor were also required to summate the two systems of different units by normalizing them. The maximum stress was selected to be under the yield strength of the steel; in addition to the maximum materials cost, these values were identified as the base values, and the revised objective function can be represented as:

$$\text{Objective function} = \Sigma(\alpha f(t, v)/f_{\max} + (1 - \alpha)g(t, v)$$

$$0 < f(t, v)/f_{\max}, \quad 0 < g(t, v)/g_{\max} \le i$$

where, α: the weight factor, $f_{\max}$: the maximum stress under the yield strength of the steel, $g_{\max}$: the maximum materials cost.

3.3. Impact test of the hybrid strut tower

A 5-kg impactor was dropped at a height of 645 mm for the impact test, and the initial impact speed and force history data were measured by a photoelectric sensor (E32-T11L and E3X-F21, Omron, Japan) and a force transducer (PCB234B, PCB, USA), respectively. A schematic diagram of the drop weight impact tester and a specimen assembled with the mechanical bolts are shown in the Figure 5. A rectangular plate was used as the impactor to apply an impulse to the three mechanical bolts at the same time. The impact energy of 31.64 J was calculated using the equation given below:

$$E = mgh$$

where, E: the impact energy, m: the total mass, g: the acceleration of gravity, h: the drop height.

The two types of specimens, the hot-rolled steel and the hybrid composite strut towers fabricated by using the stacking sequence of $[0/90/0/90]_{2s,cp}$, were tested under axial impact in a drop-mass rig. The velocity and impact energy values can be obtained as follows:

$$v(t) = \int_{t1}^{t2} \frac{F(t)}{m} dt + v_0$$

$$E(t) = \int_{t1}^{t2} F(t)v(t)dt$$

where, F: the measured force, m: the mass of the impactor, v: the velocity of the impactor, E: the total energy.

(a) A schematic of the guided drop weight impact tester.

(b) The composite front plate and the hot-rolled steel back-up plate used in the hybrid composite strut tower.
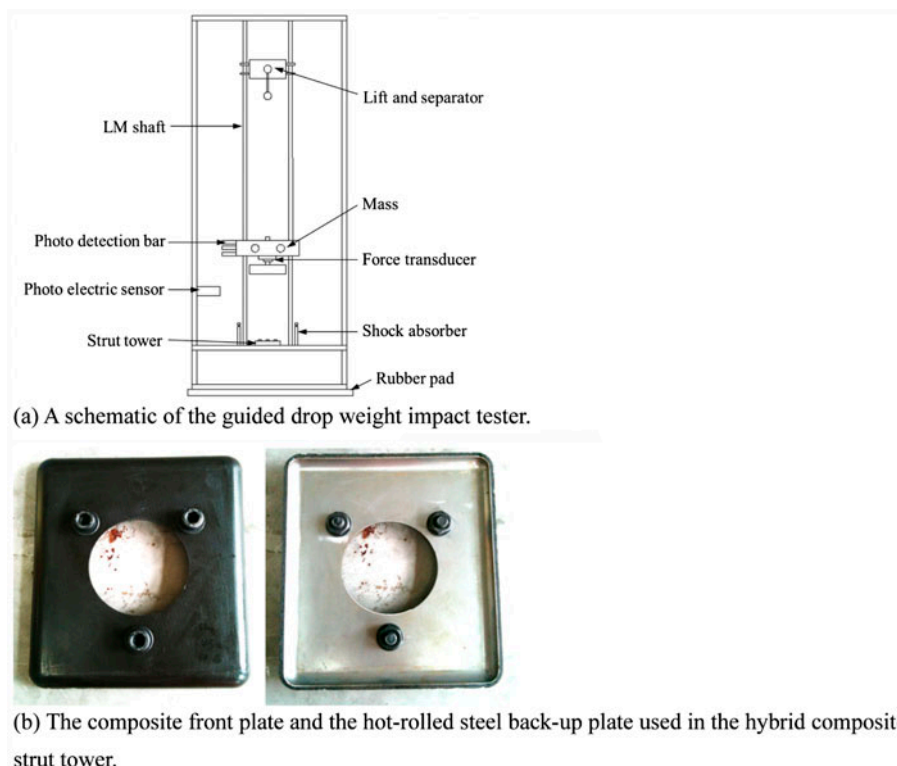
Figure 5.   The drop weight impact tester and the hybrid composite strut tower.

A 3-D measuring system (PRISMO7, Carl Zeiss, Germany) was used to investigate the permanent deflection of the hot-rolled steel strut tower before and after the impact test. Touch trigger probes were used to gather 3-D measurements of the back plate. The pathways in each of the x and y directions were measured at intervals of 10 mm, as shown in Figure 6(a). To diagnose the damage in the hybrid composite strut tower, an ultrasonic C-scanning method, which is one of the most common ways to detect damage in composites, was used because the 3-D measuring method is not suitable for detecting damage such as delamination and fiber breakage in the inner portion of the composites.

3.4.   *Dynamic analysis*

The dynamic FE-analysis based on the force and time history data of the impact test was performed to verify the static FE-analysis results. The use of raw data from the impact test can reduce the analysis time significantly; in comparison, the contact analysis caused by friction and heat energy between the impactors and the specimen are negligible. Accordingly, with respect to the load-time amplitude, the dynamic load was applied to the mechanical bolt joint of the strut tower to obtain the stress distribution. Additionally, the fundamental frequencies and the mode shapes were also calculated to study the dynamic response of the strut tower.
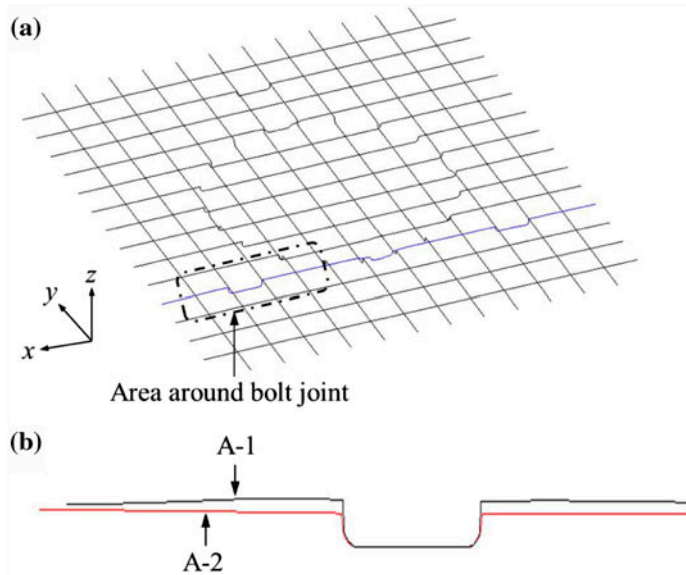
Figure 6. The 3-D measurement results of the hot-rolled steel strut tower: (a) Touch trigger probes pathways, (b) plastic deflection in the area around the bolt join of the hot-rolled steel strut tower (A-1: after the impact test, A-2: before the impact test).

3.5.   Results and discussion

The maximum stresses of the steel parts with respect to the laminate stacking sequence occurred around the bolt joint where the impact force was applied directly and Figure 3 shows the stress distribution of the hot-rolled steel tower and hybrid composite strut tower with a laminate stacking sequence of $[0/90/0/90]_{s,ce}$, whose composite part had a maximum stress in all cases.

Both the maximum stress and materials cost, with their values normalized with respect to the stacking sequence, are shown in Table 2. The total thickness of the laminate had a greater effect on the maximum stress than the laminate stiffness because the flexural stiffness determining the bending deflection is proportional to the cubic of the thickness. The materials cost significantly increased as the laminate thickness and the volume ratio of the carbon/epoxy were increased.

The calculated objective function values of each stacking sequence with respect to the weight factor are shown in Figure 7. The stacking sequence of $[0/90/0/90]_{2s,cp}$ showed a minimum value when the weight factor was apportioned equally between the normalized maximum stress and materials cost due to effect of laminate thickness and low cost of the carbon/phenolic composite. The stress and materials cost decreased by 34.6 and 37.4%, respectively, compared to the maximum values. The optimum stacking sequence fell into the pattern of $[0/90/0/90/0/90]_{s,cp}$ as the weight factor of 0.3 was given due to the cost-effectiveness, but the objective function value was not significantly different vs. that of $[0/90/0/90]_{2s,cp}$. In this case, the stress and materials cost decreased by 3.0 and 53.1%, respectively. Accordingly, the stacking sequence of $[0/90/0/90]_{2s,cp}$ was identified for fabricating the hybrid composite strut tower.

The impact force and energy absorption histories of the drop weight impact test are shown in Figure 8. The maximum force of the hot-rolled steel and hybrid composite
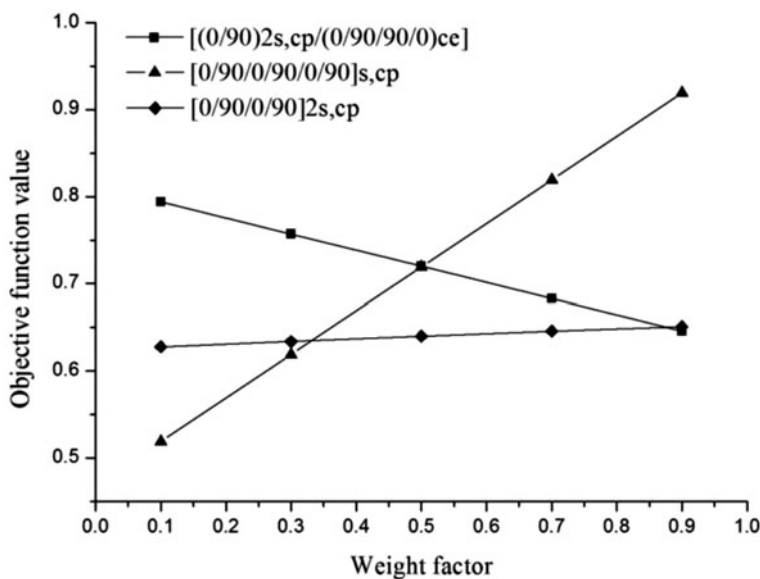
Figure 7.   The objective function values of each stacking sequence with respect to the weight factor.
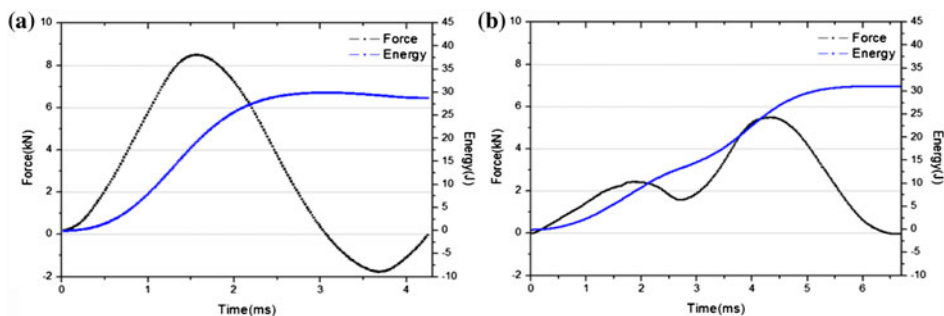

Figure 8.   The force and energy histories of the impact test: (a) the hot-rolled steel strut tower and (b) the hybrid composite strut tower.

strut towers are 8.51 and 5.50 kN, respectively, and the contact times in the positive curve are 3.06 and 6.52 ms. The maximum force of the hybrid composite strut tower was decreased by two times compared to that of the hot-rolled steel strut tower due to an increase in the contact time. In the results of the 3-D measurements, a maximum permanent deflection of 0.6 mm occurred around the bolt joints of the hot-rolled steel strut tower, as shown in Figure 6(b). The maximum force of the hot-rolled steel strut tower is very similar to the value of 8.64 kN, which was obtained by the simple dynamic calculation. This result shows that the failure of the hot-rolled steel strut tower likely occurred under the severe working conditions. In the force history of the hybrid composite strut tower, a double peak can be clearly observed at 1.82 and 4.3 ms. An observation of multiple peaks generally indicates damage, such as matrix cracking, fiber breaking, and delamination in composite materials. [17] The results of the C-scanning
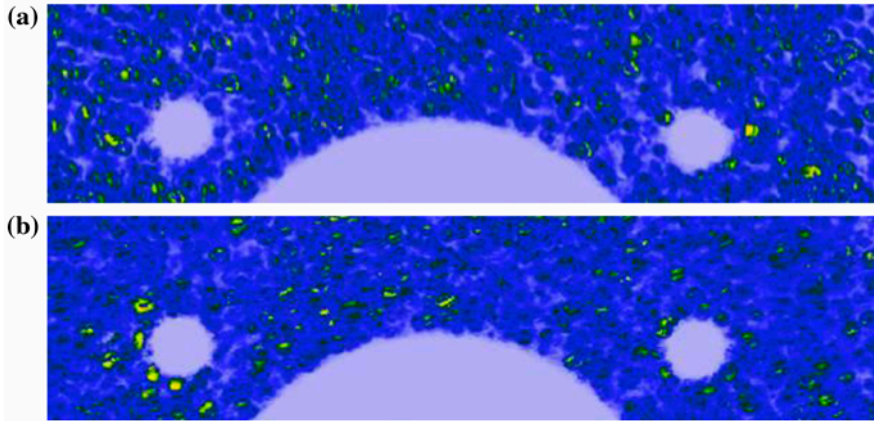
Figure 9. The ultrasonic C-scan images of the hybrid strut tower manufactured with a stacking sequence of $[0/90/0/90]_{2s,cp}$: (a) before the impact test and (b) after the impact test.

around the bolt joint of the hybrid composite strut tower, before and after the impact test, are shown in Figure 9. Any damage, such as delamination and fiber breakage, was not detected in the diagnosis through the C-scan images. The positive slope of the first curve is lower in value than that of the second curve. Thus, the double peak is caused by the difference in stiffness between the composite part and the steel part because the stiffness of hot-rolled steel is three times higher than that of the composite laminate of $[0/90/0/90]_{2s,cp}$. The hybrid composite strut tower exhibited a higher impact energy absorption capacity than that of the hot-rolled steel strut tower, as shown in Figure 8. The energy-time curve of the hot-rolled steel strut tower was decreased after the force direction was changed from positive to negative, which implies that the impactor rebounded following collision with the strut tower. Further, the rebounding of the
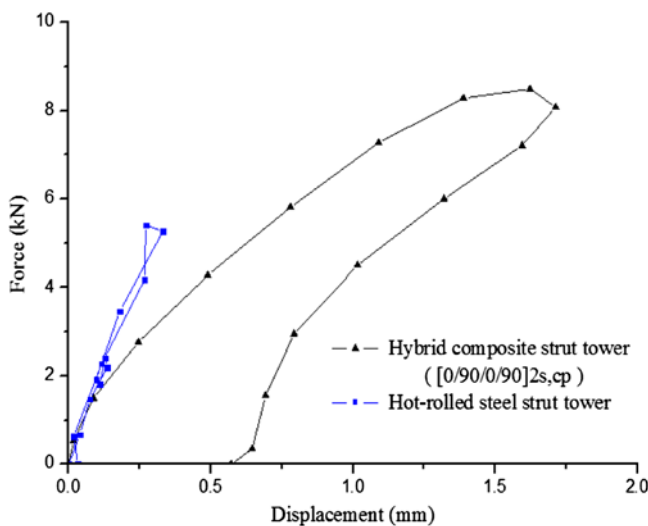

Figure 10. The load-displacement curves generated by the dynamic FE-analysis.

impactor on the hybrid composite strut tower was nearly zero. From these results, it is clear that the elastic energy absorption capacity of the hybrid composite strut tower was higher than that of the hot-rolled steel strut tower.

The force-displacement curves calculated by the dynamic FE-analysis are shown in Figure 10. When the dynamic loading fell to zero, a permanent deflection of 0.57 mm occurred around the mechanical bolt joint on the hot-rolled steel strut tower, and this value is almost the same as the result of the 3-D measurements following the impact test. In the case of the hybrid composite strut tower, any permanent deformation did not occur, which coincides with the C-scanning result. The stress distribution of the strut towers in the dynamic FE-analysis is shown in Figure 11. As a result of the static FE-analysis, the maximum stress of the hot-rolled steel strut tower exceeds the yield
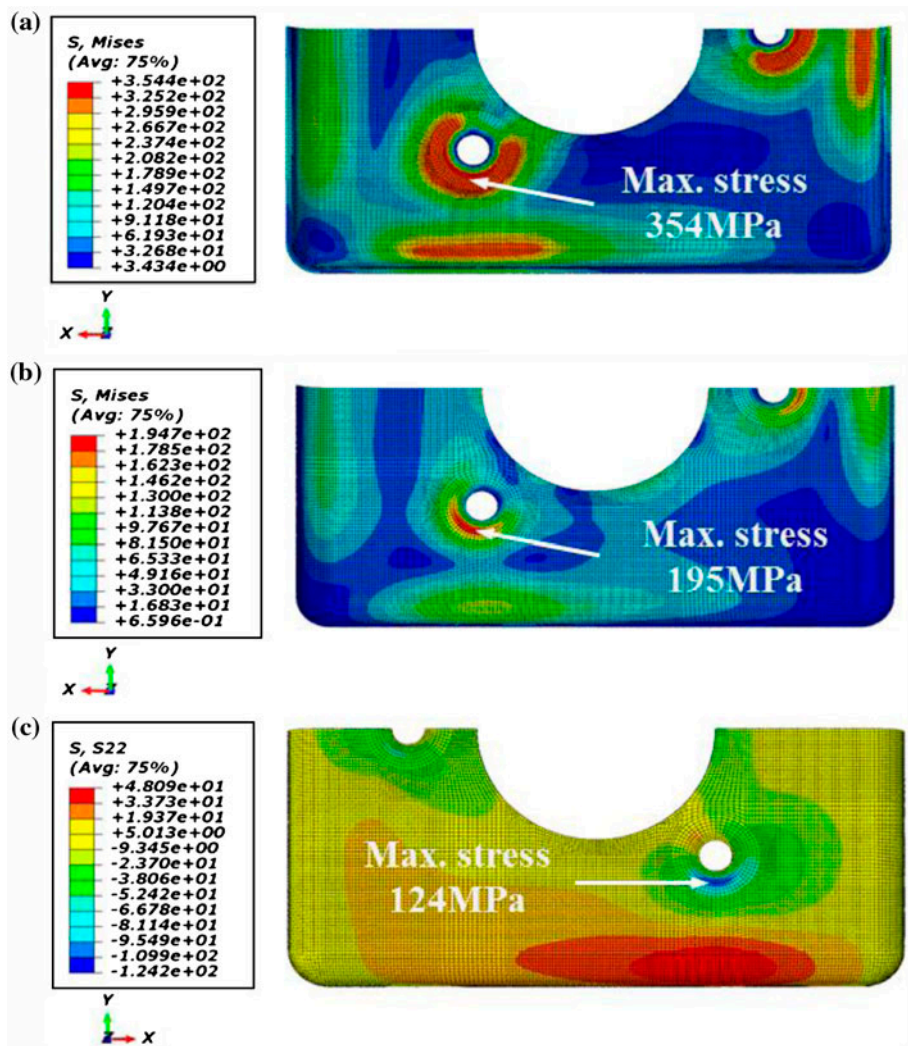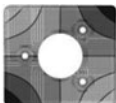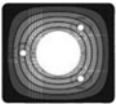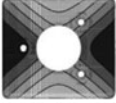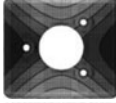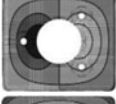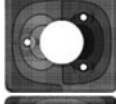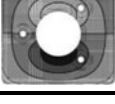

Figure 11.   The stress distribution in the hot-rolled steel strut tower and the hybrid composite strut tower with a laminate stacking sequence of $[0/90/0/90]_{2s,cp}$ in the dynamic/explicit FE-analysis: (a) the hot-rolled steel strut tower, (b) the steel part, and (c) the composite part.

Table 3. The fundamental frequencies and the mode shapes of the strut towers.

Mode No	Hot-rolled steel strut tower		Hybrid composite strut tower ([0/90/0/90]$_{2s,cp}$)	
	Mode shape	Frequency (Hz)	Mode shape	Frequency (Hz)
1		172.8		197.5
2		500.8		684.6
3		748.8		936.8
4		782.7		1144.1
5		852.6		1230.0

stress of the hot-rolled steel. The maximum stress of the hot-rolled steel part and the composite part in the hybrid composite strut tower are 195 and 124 MPa, respectively, and these values are nearly the same as the results of the static FE-analysis. The overall stress distribution and the location of maximum stress also show the same tendency. Similarly, it was found that the optimum design process of the hybrid composite strut tower for lightweight structures without any damage is valid.
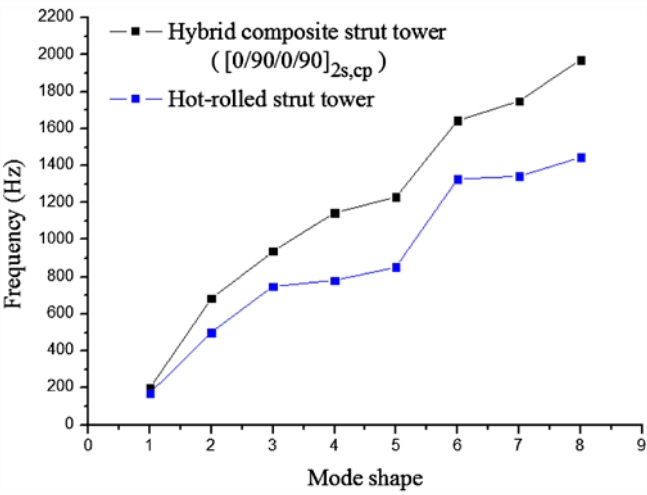

Figure 12. The fundamental frequencies of the strut tower.

The fundamental frequencies and the mode shapes of the strut towers are shown in Table 3. The mode shapes occurring from the rigid body motion of the strut tower were not contained. The first bending modes of the hot-rolled steel and the hybrid composite strut tower were observed at 500.8 and 684.6 Hz, respectively. The frequency at the first bending mode is significant because it can strongly contribute to the generation of mushrooming in the strut tower at the resonance state. Figure 12 shows that the fundamental frequencies of the hybrid composite strut tower are higher than that of the hot-rolled steel strut tower in all mode shapes. This result indicates that the structural stiffness of the hybrid composite strut tower was improved because the fundamental frequency is in proportion with the structural stiffness.

4. Conclusion

In this work, a hybrid composite strut tower for use in automobiles was fabricated of carbon fiber-reinforced composites with back-up metal and was designed to increase the structural rigidity for the prevention of permanent deflection and cracking. From the analytical and experimental results, the following conclusions were obtained:

(1) Based on the static FE-analysis, the optimum stacking sequence of the hybrid composite strut tower was $[0/90/0/90]_{2s,cp}$.

(2) The hybrid composite strut tower with a stacking sequence of $[0/90/0/90]_{2s,cp}$ was achieved as a lightweight structure of 29.2% of the weight of the hot-rolled steel strut tower.

(3) In the impact test, the maximum dynamic load of the hybrid composite strut tower was decreased by 54.7% compared to that of the hot-rolled steel strut tower.

(4) The maximum stress of the hybrid composite strut tower was decreased by 45% compared to that of the hot-rolled steel strut tower in the dynamic FE-analysis with respect to the load-time history of the impact test.

(5) Any damages and permanent deflection caused by the low-velocity impact loading were not generated in the hybrid composite strut tower fabricated with an optimum stacking sequence of $[0/90/0/90]_{2s,cp}$.

Consequently, it was found that the lightweight hybrid composite strut tower has a high potential to substitute for the conventional strut tower for the prevention of failure by impulses transferred from the road surface.

References

[1] Kim SS, Lee DG. Design of the hybrid composite journal bearing assembled by interference fit. Compos. Struct. 2006;75:223–230.

[2] Feraboli P, Masini A, Taraborrelli L, Pivetti A. Integrated development of CFRP structures for a topless high performance vehicle. Compos. Struct. 2007;78:495–506.

[3] Colombo D, Gobbi M, Mastinu G, Pennati M. Analysis of an unsual McPherson suspension failure. Eng. Fail. Anal. 2009;16:1000–1010.

[4] Park S, Popov AA, Cole DJ. Influence of soil deformation on off-road heavy vehicle suspension vibration. J. Terramech. 2004;41:41–68.

[5] Ben Mrad R, Levitt JA, Fassois SD. Non-linear dynamic modelling of an automobile hydraulic active suspension system. Mech. Syst. Signal Process. 1994;8:485–517.

[6] Minakawa M, Nakahara J, Ninomiya J, Orimoto Y. Method for measuring force transmitted from road surface to tires and its applications. JASE Rev. 1999;20:479–485.

[7] He BY, Wang SX, Gao F. Failure analysis of an automobile damper spring tower. Eng. Fail. Anal. 2010;17:498–505.

[8] Darwish SM, Ghanya A. Development of spot-weld bonded low carbon steel damping sheets. Int. MDP Conference. 2000;1:477–488.

[9] Feraboli P, Masini A. Development of carbon/epoxy structural components for a high performance vehicle. Composites Part B. 2004;35:323–330.

[10] Al-Qureshi HA. Automobile leaf springs from composite materials. J. Mater. Process. Tech. 2001;118:58–61.

[11] Choi WS, Park GJ. Structural optimization using equivalent static loads at all time intervals. Comput. Methods Appl. Mech. Eng. 2002;191:2077–2094.

[12] Lee JG. The visual method of cumulative fatigue damage by dynamic software. RecurDyn User's Conference; Seongnam; 2002.

[13] Taylor DP. Energy management utilizing the hydraulic shock absorber. Yongpyong: Taylor Devices. Technical paper; 2012.

[14] Duni E, Monfrino G, Saponaro R, Caudano M, Urbinati F. Numerical simulation of full vehicle dynamic behavior based on the interaction between Abaqus/Standard and Explicit codes. Abaqus Users' Conference; Munich; 2003.

[15] Kang S, Ok J, Yoo W, Choi J. Designing hydraulic strut mount with FSI analysis and application to a quarter car model for improving NVH performance of vehicle. New York (NY): The Korean Society of Mechanical Engineers; 2009

[16] Arora JS. Introduction to opimum design. New York, NY: McGraw-Hill; 1994.

[17] Shyr T-W, Pan Y-H. Low velocity impact responses of hollow core sandwich laminate and interplay hybrid laminate. Compos. Struct. 2004;64:I89–I98.